Steady-state hopping conduction in the conduction-band tail of a-Si:H studied in thin-film transistors

A. Nagy, M. Hundhausen, and L. Ley
Institut für Technische Physik, Universität Erlangen-Nürnberg, Erwin-Rommel-Straße 1, D-91058 Erlangen, Germany

G. Brunst and E. Holzenkämpfer
Heimann Optoelectronics GmbH, P.O. Box 3007, D-65020 Wiesbaden, Germany
(Received 23 February 1995; revised manuscript received 5 May 1995)

We have measured the temperature-dependent channel conductivity of a thin film transistor that employs hydrogenated amorphous silicon (a-Si:H) as the active layer. Two regimes of conductivity are observed. At temperatures above 100 K the conductivity is thermally activated indicating transport above the mobility edge E_C that separates localized from extended states. From the activation energy we conclude that the Fermi energy is moved as close as 62 meV towards E_C for gate voltages above 100 V. In the low-temperature regime ($T < 50$ K) the conductivity is no longer activated with a single activation energy indicating transport by hopping in the localized band tail states of a-Si:H. We present calculations of the conductivities in a model where the microscopic tunneling rates are averaged in order to obtain the energy dependent mobility. The agreement of these calculations with the data is considerably improved when a localization length of the band tail states is adopted that increases inversely with the square root of their energy below E_C.

I. INTRODUCTION

Mott showed that hopping of electrons between localized states in disordered systems gives a conductivity that depends on temperature, according to $\sigma(T) \propto \exp(-T^{-1/4})$, if the Fermi energy lies in a band of localized states having a constant density of states.[1] This law was experimentally confirmed[1] in many amorphous semiconductors, having a high density of gap states of the order of 10^{19} cm^{-3} eV^{-1}. After the discovery of the plasma enhanced chemical vapor deposition technique[2,3] for the preparation of hydrogenated amorphous silicon (a-Si:H), the density of states in the center of the gap of this material was greatly reduced below 10^{16} cm^{-3} eV^{-1}. The transport is, therefore, no longer due to hopping at E_F, but rather due to electrons that are thermally excited into delocalized states above the conduction-band edge E_C (or below the valence-band edge E_V for holes).[3]

In spite of the low density of midgap states a-Si:H has a high density of localized states that extends in the form of exponential band tails from the respective mobility edges.[4] Except for heavily phosphorus-doped a-Si:H, the Fermi energy cannot be moved into these regions such that hopping dark conductivity can be measured under steady-state conditions. However, hopping transitions between localized states in the band tails have to be considered for transient experiments.[5] If such experiments are performed at low temperatures, transport might be dominated by hopping in states at the so called transport energy E_{tr} that lies in the band tail. For transient measurements E_{tr}, in general, also depends on time.

In this paper, we demonstrate that steady-state dark-conductivity experiments in the active a-Si:H layer of thin-film transistors (TFT's) can be performed under conditions where the Fermi energy is moved so far into the conduction-band tail as cannot be realized by doping. Under these conditions, there is a clear indication of hopping conduction in band tail states, provided the Fermi level is closer than 100 meV to E_C. To reach these conditions, we apply gate voltages higher than normally used in device applications on account of the disadvantageously large shifts of the threshold voltage and the danger to destroy the TFT at room temperature.

Our conductivity data are interpreted in terms of an algorithm developed by Shapiro and Adler to calculate the temperature-dependent hopping conductivity for arbitrary density of states distributions.[6] Using that algorithm, we find that the transport path lies in the band tail at an energy E_{tr} that is time independent for our steady-state experiment. In extension of the work of Shapiro and Adler, we include an energy dependent localization length of the states involved in the hopping transitions.

This paper is organized as follows. After giving experimental details in Sec. II, we describe the hopping model used for the calculations in Sec. III. The experimental results and their comparison with the calculations are given in Sec. IV and we conclude in Sec. V.

II. EXPERIMENTAL DETAILS

A. Sample

For this study, we have used an a-Si:H thin-film transistor deposited on Corning 7059 substrates at a deposition temperature of 250 °C. The TFT configuration is basically the same as in Fig. 3.18 of Ref. 7. The Cr gate was separated from the channel by a 400 nm thick layer

of amorphous hydrogenated silicon nitride, a-SiN_x:H. For the active layer, undoped a-Si:H with a thickness of 250 nm was deposited and for the drain and source contacts n^+ a-Si:H layers with Cr contacts were deposited on top of the active layer. Channel length and width were 250 μm and 1 mm, respectively.

For the calculation of the geometry factor relating conductivity with conductance in our device, we need an estimation of the channel thickness. This is done as follows. At the TFT junction, there is a band bending induced by the gate voltage. As a result, not only the energy difference between the Fermi energy E_F and the conduction-band edge $E_C(x)$, but also the space charge $\rho(x)$ and the density of band tail states $g_{\rm bt}(E,x)$ depend on the spatial coordinate x, that is the distance to the silicon-silicon nitride interface. The two-dimensional charge density in the TFT channel Q_{2d} is obtained by integrating $\rho(x)$ according to

$$Q_{2d} = \int_0^{d_{\rm Si}} \rho(x) dx, \tag{1}$$

where $d_{\rm Si}$ corresponds to a thickness of the a-Si:H layer that includes the channel. $\rho(x)$ can be calculated by integrating the charge residing in band tail states, which is in the T=0 approximation,

$$\rho(x) = e \int_{-\infty}^{E_F} g_{\rm bt}(E,x)\, dE. \tag{2}$$

Substituting Eq. (2) into Eq. (1), we obtain

$$Q_{2d} = e \int_0^{d_{\rm Si}} \int_{-\infty}^{E_F} g_{\rm bt}(E,x)\, dE\, dx. \tag{3}$$

We approximate the band bending of $E_C(x)$ with a step function,

$$E_C(x) \approx \begin{cases} E_F + \Delta E_{\rm a,exp} & \text{for } 0 \le x \le d_{\rm eff} \\ E_{C,0} & \text{for } x > d_{\rm eff}, \end{cases} \tag{4}$$

where $\Delta E_{\rm a,exp}$ is the experimentally observed conductivity activation energy, $d_{\rm eff}$ is the effective channel thickness that is chosen to give the correct value of Q_{2d}, and $E_{C,0}$ is the value of the conduction-band edge far from the interface. If we use Eq. (4), the contribution to Q_{2d} is negligible for $x > d_{\rm eff}$, so that Eq. (3) becomes

$$Q_{2d} = e \int_{-\infty}^{E_C - \Delta E_{\rm a,exp}} g_{\rm bt}(E)\, dE d_{\rm eff}, \tag{5}$$

where we have used Eq. (4) to substitute for E_F in the upper limit of integration. Also, we note that $g_{\rm bt}(E,x)$ and $E_C(x)$ are independent of x over the range of interest, $0 \le x \le d_{\rm eff}$, and, therefore, x has been dropped from the notation. The effective space charge density in the channel can be calculated from $\Delta E_{\rm a,exp}$, using the density of states defined below in Eq. (16). The two-dimensional space charge density in the channel also relates to the voltage applied to the gate corrected for the threshold voltage and the band bending in the silicon ($U^*_{\rm SiN_x}$) according to

$$Q_{2d} = \frac{U^*_{\rm SiN_x}}{d_{\rm SiN_x}} \epsilon_0 \epsilon_{\rm SiN_x}, \tag{6}$$

where $d_{\rm SiN_x}$ = 400 nm and $\epsilon_{\rm SiN_x}$=5.8 are, respectively, the thickness and dielectric constant of the a-SiN_x layer. We obtain $d_{\rm eff}$ from Eqs. (5) and (6) to lie between 4 nm and 7 nm, when the gate voltage is varied between 100 V and 30 V.

B. Measurements

Dark-conductivity measurements were carried out in a He cryostat at temperatures between 12 K and 250 K. The gate voltage U_g was varied between 10 V and 120 V. For high gate voltages, we observed a significant shift of the threshold voltage $U_{\rm th}$ of the TFT, due to field induced charge injection into the gate insulator.[8] At the highest gate voltages employed, $U_{\rm th}$ was as high as 30 V. After each measurement, we checked that $U_{\rm th}$ had not changed significantly during the measurement. We found that threshold voltage shifts, due to high gate voltages, were larger at higher temperatures. Nickel *et al.* reported defect creation in the active a-Si:H layer of TFT's, due to high gate voltages.[9] Because the efficiency of that process is thermally activated with an activation energy of 0.7 eV, the defect creation is negligible at low temperature. Therefore, we applied gate voltages above 10 V at temperatures below 250 K only.

At low temperatures (T < 50 K), we measured the I-V characteristics between source-drain current $I_{\rm sd}$ and source-drain voltage $U_{\rm sd}$ for fixed U_g. $I_{\rm sd}$ was very small below an onset $U_{\rm sd}$ of about 9 V and increased linearly with $U_{\rm sd}$ above that voltage. We attribute this behavior to the nonlinear characteristics of the source and drain contacts that lie in series with the TFT-channel resistance. We assign the main contribution to the low-temperature contact resistance to the intrinsic a-Si:H layer separating the n^+ layer and the channel. Nebel and Street have measured the I-V characteristics of n^+-i-n^+ structures at low temperatures and found that the conductivity σ shows a strongly nonlinear dependence on electric field F in the range $1.5 \sim 3 \times 10^5$ V/cm according to a power law [$\sigma \propto F^y$, $(14 < y < 17)$].[10] They attributed this behavior to space charge limited currents. Our observation of an onset source-drain voltage is in agreement with their data, since a voltage drop of 9 V over the two contact regions implies electric fields of 1.8×10^5 V/cm. As a result of the steep overlinear decrease of the contact resistance with field, the voltage drop is rather constant for $U_{\rm sd}$ > 9 V, since the channel resistance is Ohmic. Consequently, we use an effective source-drain voltage $U^*_{\rm sd} = U_{\rm sd} - 9$ V, in this paper, in order to calculate the channel conductivity. We find that the channel conductivity so calculated is independent of the choice of $U^*_{\rm sd}$, as long as $U^*_{\rm sd} \gtrsim 1$ V. The low-temperature data presented here were measured at $U_{\rm sd}$=15 V. Note that the voltage drop over the contact region was negligible at around room temperature, due to the higher conductivity of the intrinsic layer.

III. HOPPING MODEL

At high temperatures the conductivity of the TFT channel is thermally activated, suggesting that electronic transport is due to electrons thermally excited above the mobility edge in this case. At low temperatures ($T \lesssim 50$ K) however, the conductivity is no longer thermally activated and much higher than expected from the activation energy determined at higher temperatures. We ascribe the excess low-temperature conductivity to hopping conduction and we are going to fit our results to model calculations that we performed with the algorithm described by Shapiro and Adler.[6] This model allows for a calculation of the temperature-dependent conductivity with arbitrary density of states distributions. By using this model, we implicitly ignore the band bending at the TFT junction and replace the inhomogeneous charge density distribution by a constant effective space charge density in the whole channel having an effective thickness d_{eff}. We, thus, also assume a constant energy difference between E_C and the Fermi energy that we relate below to the conductivity activation energy. We expect that this simplification has only little effect on the calculated conductivity, since it ignores the contribution of electrons trapped further away from the TFT junction. These electrons reside in states deeper in the band tail, due to the band bending, thus giving only a minor contribution to the conductance as compared to electrons right at the TFT junction.

The conductivity $\sigma(T)$ is calculated by integration of the differential conductivity $\sigma(E,T)$ over energy according to

$$\sigma(T) = \int \sigma(E,T)dE = \int e g_{\text{bt}}(E) f(E) \mu(E) dE, \quad (7)$$

where e is the electron charge, g_{bt} the density of localized states in the conduction-band tail of the active layer material, $f(E) = 1/\{1 + \exp[(E - E_F)/k_BT]\}$ the Fermi distribution function, and $\mu(E)$ the energy and temperature-dependent hopping mobility. Note that the quantities $f(E)$ and $\mu(E)$ implicitly also depend on temperature. The mobility relates to the diffusion constant $D(E)$ via Einstein's equation:

$$\mu(E) = D(E)\frac{e}{k_BT}. \quad (8)$$

Microscopically, the diffusion constant is determined by the transition rate from an occupied state i to an unoccupied state j that depends on their spatial and energetical distance according to

$$D_{ij} = \frac{R_{ij}^2}{6}\nu_{ij} = \frac{R_{ij}^2}{6}\nu_0 \exp\left(\frac{-2R_{ij}}{\alpha}\right) \times \begin{cases} \exp\left(\dfrac{E_i - E_j}{k_BT}\right) & \text{for } E_j \geq E_i \\ 1 & \text{for } E_j < E_i. \end{cases} \quad (9)$$

Here, E_i and E_j are the energies of the initial and final state, respectively, R_{ij} is their spatial separation, α the localization length of the states involved, and ν_0 the attempt frequency. For ν_0, a range 10^{12} s^{-1} $< \nu_0 <$ 10^{13} s^{-1} is generally assumed and we are going to use $\nu_0 = 3 \times 10^{12}$ s^{-1} here.

The task of calculating $\sigma(E,T)$ is the averaging of the D_{ij} over the whole sample volume with $E_i = E$. This is performed in the model of Shapiro and Adler by using an average hopping distance $\overline{R}(E)$ defined in terms of the concentration of available final states N_f, according to

$$\overline{R}(E) = N_f^{-1/3}. \quad (10)$$

N_f is divided into one part $N_1(E)$ corresponding to empty states having an energy below E and a fraction of states $N_2(E)$ having an energy higher than E:

$$N_f = N_1(E) + N_2(E). \quad (11)$$

The argument E indicates that the integral quantities N_1 and N_2 depend on energy E of the initial states. $N_1(E)$ is calculated by integration over all unoccupied states below E:

$$N_1(E) = \int_{-\infty}^{E} g_{\text{bt}}(E')\,[1 - f(E')]\,dE'. \quad (12)$$

For hops to states with energy E' above E, the density of available empty states, $g_{\text{bt}}(E')$, is weighted with the appropriate Boltzmann factor to account for the number of phonons necessary to provide the energy $E' - E$:

$$N_2(E) = \int_{E}^{\infty} g_{\text{bt}}(E')\,[1 - f(E')] \exp\left(\frac{E - E'}{k_BT}\right) dE'. \quad (13)$$

With the average hopping distance $\overline{R}(E)$ so obtained, the diffusion constant $D(E)$ is calculated according to

$$D(E) = \frac{\overline{R}^2(E)}{6}\nu_0 \exp\left[\frac{-2\overline{R}(E)}{\alpha}\right]. \quad (14)$$

Below, we are going to test two alternatives for the localization length α, namely, an energy independent α and an $\alpha(E)$ that depends on energy according to

$$\alpha(E) \propto (E_C - E)^{-0.5}. \quad (15)$$

This law was suggested by Abram and Edwards albeit with an exponent that was –0.6 for shallow states and –0.5 for deeper states.[11] Equation (15) implies that the localization length is inversely proportional to the square root of the energy of the state measured from the energy of the mobility edge E_C. Since D depends exponentially on α^{-1}, it is readily conceivable that this energy dependence considerably influences the energy dependent mobility and hence the conductivity. Thus, we include $\alpha(E)$ into the hopping algorithm by replacing Eq. (14) with

$$D(E) = \frac{\overline{R}^2(E)}{6}\nu_0 \exp\left[\frac{-2\overline{R}(E)}{\alpha(E)}\right]. \quad (14')$$

In this equation, we use the localization length of the ini-

tial states at the energy E. This is correct for transitions to states with energy below E that are more strongly localized, but is an approximation for hopping transitions to energetically higher final states (i.e., states that have a larger α). Note, that for transitions between two states with different α in Eq. (9) the more extended wave function dominates the transition rate when the hopping distance is large compared to α.[12]

For the density of states of the conduction-band tail $g_{\rm bt}$, we assume an exponential energy distribution for energies more than 70 meV below E_C and a linear distribution above that energy.[13,14] The parameters are chosen so that the derivative of $g_{\rm bt}$, with respect to E, is equal at the transition energy E_m from one regime to the other:

$$g_{\rm bt}(E) = N_{0,C} \times \begin{cases} \exp\left(\dfrac{E-E_C}{E_{0,C}}\right) & \text{for } E < E_m \\ \exp\left(\dfrac{-0.07\text{eV}}{\text{E}_{0,\text{C}}}\right)\left[1+\dfrac{E-E_m}{E_{0,C}}\right] & \text{for } E \geq E_m, \end{cases} \quad (16)$$

with $E_{0,C}$=25 meV, $E_m = E_C - 0.07$ eV, and $N_{0,C} = 8.65\times10^{21}$ cm^{-3} eV^{-1}. Also, the parameters were chosen to be consistent with Fig. 6 of Ref. 14, where the density of states at the mobility edge is $g_{\rm bt}(E_C)$=2×10^{21} cm^{-3} eV^{-1}.

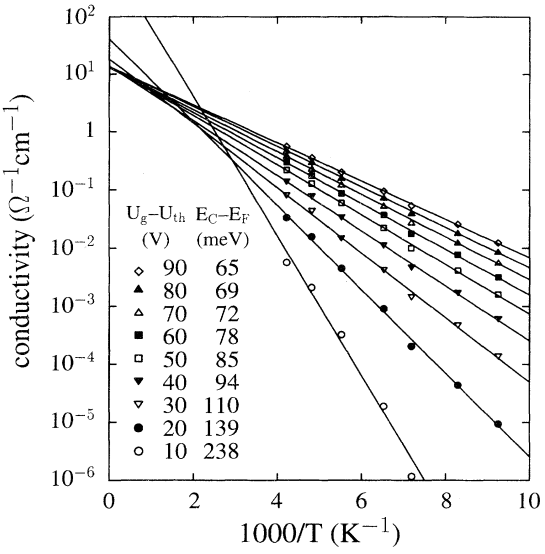

FIG. 1. Arrhenius plot of the TFT-channel conductivity as a function of inverse temperature for different gate voltages. The lines are least square fits of the data to thermally activated conductivity. The corresponding activation energies $E_C - E_F$ are given together with the gate voltages applied to the gate metal minus the measured threshold voltages.

IV. RESULTS AND DISCUSSION

A. High-temperature regime

The conductivity of our TFT is shown in the high-temperature regime (100 K$\leq T \leq$ 250 K) in an Arrhenius plot in Fig. 1 for corrected gate voltages ($U_g - U_{\rm th}$) ranging from 10 V to 90 V. For each gate voltage, the data are well described in terms of a thermally activated conductivity as is commonly found in device-quality a-Si:H. This indicates transport above the mobility edge E_C. We interpret the measured activation energies as the energy difference between the Fermi energy E_F and E_C. We estimate that deviations between the measured activation energy and $E_C - E_F$, due to a statistical shift of E_F, are negligible for the temperature range discussed in Sec. IV B below. The Fermi energy is moved as close as 65 meV towards E_C for the highest gate voltage employed in Fig. 1 ($U_g - U_{\rm th} = 90$ V).

The conductivity prefactors σ_0 (i.e., the conductivity extrapolated to $1/T$=0) obtained from Fig. 1 are constant ($\sigma_0 \approx 10\ \Omega^{-1}$ cm^{-1}) for $E_C - E_F$ <100 meV and increase only for larger activation energies. Hence, it appears that the Meyer-Neldel rule,[15] i.e., the linear relationship between $\ln(\sigma_0)$ and the activation energy does not hold for activation energies below 100 meV. This finding is supported by the theory of Overhof and Thomas,[7] who attribute the Meyer-Neldel rule to be due to the statistical shift of E_F. They find a minimum and consequently a weak activation energy dependence of the conductivity prefactor at around $E_F - E_C$=100 meV.

B. Low-temperature regime

In Fig. 2(a), the conductivities of the TFT are shown for temperatures between 16 K and 100 K in an Arrhenius plot with the gate voltage as parameter. Gate voltages $U_g - U_{\rm th}$ between 23 V and 100 V correspond to Fermi level positions between 128 meV> $E_C - E_F$ > 62 meV, as determined from the activation energies at higher temperatures (see Fig. 1). It is obvious that the conductivities are no longer activated with a single activation energy in that temperature range and that they are considerably larger than the values extrapolated from higher temperatures. This is especially true for the highest gate voltages used, i.e., for E_F closest to E_C. Also shown in Fig. 2(a) as lines is the sum of the extrapolated conductivity for transport in extended states and the contribution due to hopping: $\sigma_{\rm ext} + \sigma_{\rm hop}$. For the calculation of $\sigma_{\rm hop}$, we used the theory described in Sec. III, under the assumption of a constant (i.e., energy independent) localization length. The only adjustable parameter was α and it was chosen to be α = 6.5 Å, so as to give the best agreement with the experimental data for the lowest temperatures and for the lowest activation energy of 62 meV. Although the general trend of the conductivity vs gate voltage appears to be reproduced, the fit is not very good. The hopping theory with a constant α gives a sharper transition between the transport regime in extended states and the hopping regime than is experimentally observed.

In Fig. 2(b), we show a comparison of calculated conductivities with the same set of experimental data as in Fig. 2(a), but this time using an energy dependent localization length according to Eq. (15) for the theoretical curves. It is apparent that the experimental data are now well reproduced by the theory for all gate voltages. Note that only a single parameter was adjusted to obtain this agreement for the whole set of data. The relation that was used for $\alpha(E)$ to get the fit of Fig. 2(b) is

$$\alpha(E) = 1.7\ \text{Å} \left(\frac{E_C - E}{0.8\ \text{eV}} \right)^{-0.5} . \qquad (17)$$

This $\alpha(E)$ is valid for the choice of g_{bt} given in Eq. (16). When scaling g_{bt} with a constant factor, we obtain identical fits as in Fig. 2(b) if $\alpha(E)$ is rescaled so that $\alpha g_{\text{bt}}^{1/3}$ remains unchanged.

C. The differential conductivity

In order to analyze the reason for the better reproduction of the experimentally observed conductivity by the hopping theory when the localization length is assumed to depend on energy according to Eq. (17), we are going to discuss the differential conductivity $\sigma(E,T)$. To be specific, we consider $\sigma(E,T)$ for one gate voltage ($U_g - U_{\text{th}} = 80$ V) and for three temperatures. The inset of Fig. 3 sketches the density of states distribution as defined in Eq. (16) and in Fig. 4(a), we show the two alternatives for $\alpha(E)$ that were used to fit the data in Fig. 2(a) and Fig. 2(b), respectively. Figure 3 gives again the Arrhenius plot of the data for E_C–E_F= 69 meV, together with the two theoretically obtained conductivities ($\sigma_{\text{ext}} + \sigma_{\text{hop}}$). The dashed curve is that obtained with $\alpha = 6.5$ Å, and the solid curve is that calculated with $\alpha(E)$ following Eq. (17). Three characteristic temperatures shown by dots in Fig. 3 are chosen for a further discussion of the transport: For T_2=30 K and T_3=20 K, σ_{ext} is negligibly small, whereas for T_1=50 K σ_{ext} is not negligible. In Figs. 4(b)–(d), we have plotted for each of these temperatures the differential conductivity $\sigma(E,T)$, as a function of energy. The extended state differential conductivity above E_C was calculated with the assumption of a constant mobility and a constant density of states and it decays exponentially above E_C, due to the Fermi function cutoff. As expected, transport at E_C decreases with decreasing temperature [compare Fig. 4(b) with Figs. 4(c) and 4(d)]. The differential conductivity in localized states below E_C is less temperature dependent and consequently dominates at low temperatures. A maximum in $\sigma(E,T)$ is observed at energies

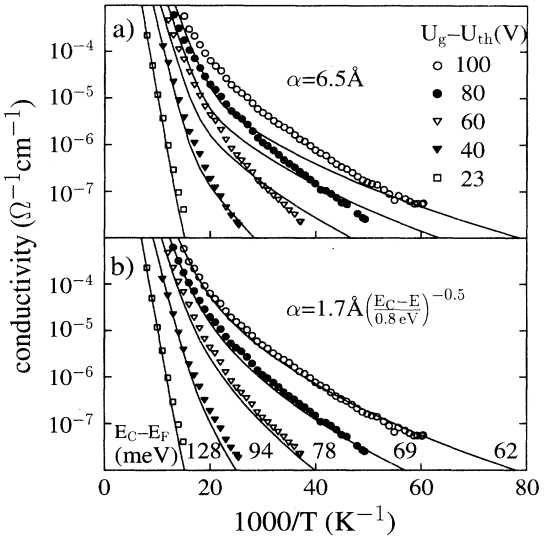

FIG. 2. Arrhenius plot of the TFT-channel conductivity for different gate voltages. The corrected gate voltages $U_g - U_{\text{th}}$ and the corresponding high-temperature dark-conductivity activation energies are given as parameters in the upper and lower figure, respectively. The same set of experimental data is shown in (a) and (b), as symbols together with different fits. (a) The curves are the sum of the extrapolated activated conductivity and the calculated hopping conductivity according to the model of Shapiro and Adler assuming a constant localization length ($\alpha = 6.5$ Å). Note, that the experimentally observed smooth transition between the low-temperature range and the higher-temperature range is not reproduced by the calculation. (b) Calculations according to Shapiro and Adler, this time using an energy dependent $\alpha(E)$ as given in the figure.

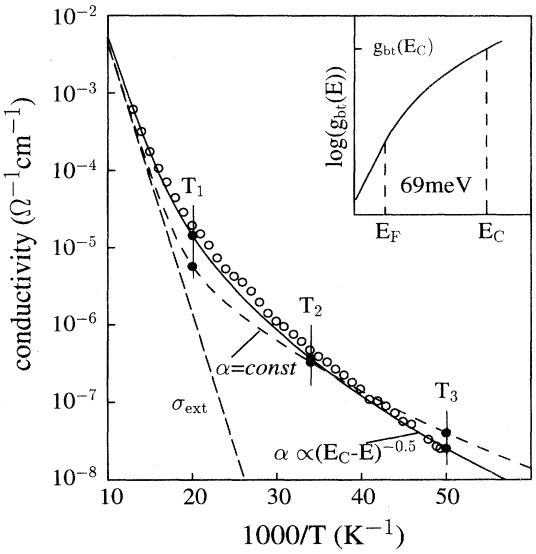

FIG. 3. Arrhenius plot of the TFT-channel conductivity for $U_g - U_{\text{th}}$=80 V. Open circles are the measured data. The solid curve is the calculated conductivity ($\sigma_{\text{ext}} + \sigma_{\text{hop}}$) for a localization length $\alpha(E)$ that depends on energy according to Eq. (17), whereas the dashed curve is the calculated conductivity for a constant $\alpha = 6.5$ Å. Note, that the fit is considerably improved for the energy dependent localization length. Filled dots mark the temperatures T_1, T_2, and T_3 at which the differential conductivities of Fig. 4 were calculated. The inset sketches the density of states distribution used in the calculation.

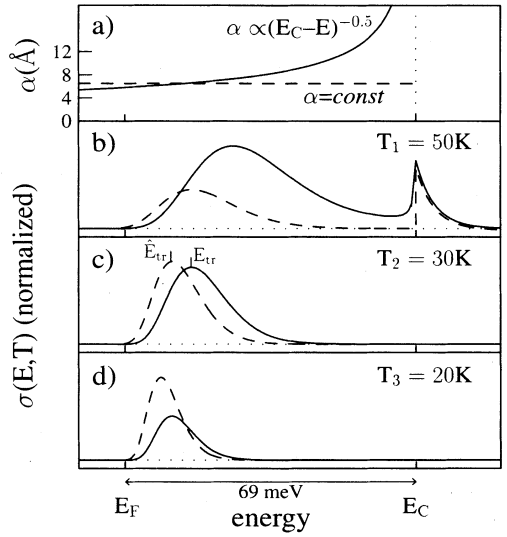

FIG. 4. (a) Two choices of localization length vs energy that were used for the model calculations of Fig. 2(a) and Fig. 2(b), respectively. The dashed and solid lines give the constant $\alpha = 6.5$ Å and $\alpha(E)$ according to Eq. (17), respectively. (b)–(d) Differential conductivities calculated for 50 K, 30 K, and 20 K. The maxima of the differential conductivity define the transport energies $E_{\rm tr}$ (variable α) and $\hat{E}_{\rm tr}$ (fixed α), respectively. The transport energy moves towards E_C with increasing temperature [see (b)–(d)]. Note that $E_{\rm tr}$ is larger than $\hat{E}_{\rm tr}$, due to the fact that α increases with energy in the first case.

$E_{\rm tr}$ (variable α) and $\hat{E}_{\rm tr}$ (constant α), the transport energies. $E_{\rm tr}$ ($\hat{E}_{\rm tr}$) increases with increasing temperature and we find $E_{\rm tr} - E_F \approx 6k_BT$ ($\hat{E}_{\rm tr} - E_F \approx 4k_BT$). The existence of a maximum is due to the fact that $\sigma(E,T)$ is the product of the Fermi function that falls off with increasing energy and the density of states and the mobility that increase with energy.[16] The increase of $\mu(E)$ is sharp, because the density of states distribution enters exponentially via $\overline{R}(E)$ [see Eq. (14)]. It is obvious from Figs. 4(b)–(d) that the increase of α when approaching E_C favors transport at higher energies. The reason for the better fit of the experimental data can now be understood; when the temperature increases, $E_{\rm tr}$ shifts higher up in the band tail, where α becomes larger. This in turn gives a larger $\sigma(E,T)$ and hence a larger $\sigma(T)$, as compared to a constant α, due to its exponential dependence in Eqs. (14) and (14′). As a consequence, the sharp transition region between hopping transport and transport in extended states is smoothed out (see Fig. 3).

To avoid confusion, we mention here that we find a temperature dependence of $E_{\rm tr}$ that differs from that given in Refs. 5 and 17, namely,

$$E'_{\rm tr} = E_C - 3E_{0,C} \ln\left(\frac{3\alpha N_{\rm exp}^{1/3} E_{0,C}}{2k_BT}\right),$$

where $N_{\rm exp}$ is the total density of localized states in a purely exponential conduction-band tail. However, that result was obtained without consideration of the occupation function and is only applicable if E_F is deep in the band tail, i.e., $E_F < E'_{\rm tr}$. Inserting typical numbers, we get $E'_{\rm tr} \lesssim E_C$–100 meV for $T < 50$ K. Consequently, the condition for application of the simplified formula of Ref. 5 is not fulfilled for the high gate voltages (and the small activation energies) employed in this work.

V. CONCLUSION

The low-temperature conductivity of the amorphous silicon layer in the channel of a thin-film transistor shows a clear indication of hopping in the band tail, when the gate voltage is chosen so high as to obtain high-temperature dark-conductivity activation energies smaller than 100 meV. Under the assumption of an energy independent localization length of all states in the band tail, only the general trends of conductivity with temperature and gate voltage can be reproduced. Quantitative agreement of our data with the transport algorithm of Shapiro and Adler is achieved if the latter is extended to allow for a variable localization length $\alpha(E)$ that is inversely proportional to the square root of the state's energy below the band edge.

[1] N. F. Mott and E. A. Davis, *Electronic Processes in Non-crystalline Materials* (Oxford University Press, Oxford, 1979).
[2] R. C. Chittik, J. H. Alexander, and H. F. Sterling, J. Electrochem. Soc. **116**, 77 (1969).
[3] W. E. Spear and P. G. LeComber, Solid State Commun. **17**, 1193 (1975).
[4] R. A. Street, *Hydrogenated Amorphous Silicon* (Cambridge University Press, Cambridge, England, 1991).
[5] D. Monroe, Phys. Rev. Lett. **54**, 146 (1985).
[6] F. R. Shapiro and D. Adler, J. Non-Cryst. Solids **77&78**, 139 (1985).
[7] H. Overhof and P. Thomas, in *Electronic Transport in Hydrogenated Amorphous Semiconductors*, edited by G. Höhler, Springer Tracts in Modern Physics Vol. 114 (Springer, Heidelberg, 1989), p. 129.
[8] M. J. Powell, Appl. Phys. Lett. **43**, 597 (1983).
[9] N. Nickel, W. Fuhs, and H. Mell, Philos. Mag. B **61**, 251 (1990).
[10] C. E. Nebel and R. A. Street, Philos. Mag. B **67**, 721 (1993).
[11] R. A. Abram and S. F. Edwards, J. Phys. C **5**, 1183 (1972).
[12] D. K. Biegelsen, R. A. Street, and W. B. Jackson, Physica **117B&118B**, 899 (1983).
[13] M. Stutzmann, D. K. Biegelsen, and R. A. Street, Phys. Rev. B **35**, 5666 (1987).

[14] C. E. Nebel, R. A. Street, N. M. Johnson, and J. Kocka, Phys. Rev. B **46**, 6789 (1992).
[15] W. Meyer and H. Neldel, Z. Tech. Phys. **12**, 588 (1937).
[16] M. Grünewald and P. Thomas, Phys. Status Solidi B **94**, 125 (1979).
[17] F. R. Shapiro and D. Adler, J. Non-Cryst. Solids **74**, 189 (1985).